Bandwidth and Resolution Enhancement Through Pulse Compression

Michael L. Oelze, *Member, IEEE*

***Abstract*—A novel pulse compression technique is developed that improves the axial resolution of an ultrasonic imaging system and provides a boost in the echo signal-to-noise ratio (eSNR). The new technique, called the resolution enhancement compression (REC) technique, was validated with simulations and experimental measurements. Image quality was examined in terms of three metrics: the eSNR, the bandwidth, and the axial resolution through the modulation transfer function (MTF). Simulations were conducted with a weakly-focused, single-element ultrasound source with a center frequency of 2.25 MHz. Experimental measurements were carried out with a single-element transducer (f/3) with a center frequency of 2.25 MHz from a planar reflector and wire targets. In simulations, axial resolution of the ultrasonic imaging system was almost doubled using the REC technique (0.29 mm) versus conventional pulsing techniques (0.60 mm). The −3 dB pulse/echo bandwidth was more than doubled from 48% to 97%, and maximum range sidelobes were −40 dB. Experimental measurements revealed an improvement in axial resolution using the REC technique (0.31 mm) versus conventional pulsing (0.44 mm). The −3 dB pulse/echo bandwidth was doubled from 56% to 113%, and maximum range sidelobes were observed at −45 dB. In addition, a significant gain in eSNR (9 to 16.2 dB) was achieved.**

I. Introduction

Coded excitation and pulse compression were first used in radar to significantly improve the echo signal-to-noise ratio (eSNR) over conventional pulsing techniques [1]–[3]. The increase of eSNR through coded excitation comes about by increasing the time-bandwidth product (TBP) through longer time signals than conventional pulsing techniques. The increase in eSNR increases the detection range of radar without appreciable loss in resolution.

Coded excitation techniques have been adapted successfully to ultrasonic imaging for the purpose of increasing the eSNR without increasing the acoustic pressure [4]–[6]. The improvement of eSNR allows for deeper penetration of ultrasonic waves and improved image quality.

Use of higher excitation voltages with conventional pulsing techniques to increase acoustic pressure is another means to improve eSNR. However, increased acoustic pressures carry with them greater potential for ultrasound-induced bioeffects, and as a result, greater patient risk [7]. One important benefit of using coded excitation to improve eSNR, while maintaining lower acoustic pressures, is that the possibility of bioeffects caused by higher-pressure ultrasonic waves can be reduced.

One detriment to implementing pulse compression techniques into ultrasonic imaging is the introduction of sidelobes [4], [8], [9]. Depending on the coding technique, sidelobes with levels as high as −13 dB can occur, e.g., coding with linear FM chirps without tapering, significantly reducing contrast resolution and image quality. One author [6] suggested that ultrasound medical imaging requires sidelobe levels less than −45 dB for acceptable image quality. Much attention has been paid to the filtering of signals and choosing appropriate coding techniques in order to reduce sidelobe levels using pulse compression [4], [6], [8]–[12]. As a result, pulse compression techniques look promising for improving the eSNR and depth-of-penetration for clinical ultrasonic imaging devices. However, the improvement in eSNR through coded excitation often comes at the expense of axial resolution.

Pulse compression using FM chirps and pulse-modulated (PM) codes also were examined recently in the context of advanced ultrasonic imaging techniques. One advanced ultrasonic imaging technique that has made use of pulse compression is ultrasound strain imaging. Liu and Insana [12] and Liu *et al.* [13] adapted coded excitation and pulse compression techniques to improve strain imaging. Strain image noise was reduced significantly using Golay complimentary codes and chirps, and the effective depth-of-focus for strain imaging was doubled.

Other advanced ultrasonic imaging techniques will benefit from coded excitation techniques. Quantitative ultrasound (QUS) techniques that parameterize the backscattered power spectrum, i.e., estimation of scatterer properties from radio-frequency (RF) signals, could be improved by increasing the eSNR. Larger eSNR may result in decreased variance of QUS estimates, larger useable bandwidth, and increased depth-of-penetration for obtaining estimates. The useable bandwidth is defined in this study as the portion of the backscattered power spectrum that is 6 dB above the noise.

Further improvements in accuracy and precision of scatterer property estimates would occur if coded excitation techniques could be used to increase the available bandwidth of the imaging system [14], [15]. Studies by Chatuverdi and Insana [14] indicated that the variance in QUS estimates (i.e., scatterer size) was inversely proportional to the bandwidth of the imaging system. Larger bandwidth

Manuscript received June 26, 2006; accepted November 13, 2006. This work was supported by start-up funds from the Department of Electrical and Computer Engineering at the University of Illinois at Urbana-Champaign.

The author is with the Department of Electrical and Computer Engineering, University of Illinois at Urbana-Champaign, Urbana, IL 61801 (e-mail: oelze@uiuc.edu).

Digital Object Identifier 10.1109/TUFFC.2007.310

leads to reduced variance in scatterer property estimates. Reduced variance in turn leads to better diagnostic capability in QUS imaging techniques and a greater ability to measure smaller differences between different kinds of tissues based on their scatterer properties. One way to increase the useable bandwidth is to increase the eSNR, which is achievable through coded excitation techniques.

Alternatively, increasing the useable bandwidth of the imaging system also may be accomplished through specialized FM chirps and pulse compression. Raman and Rao [16] and Venkatraman and Rao [17] suggested that specialized FM chirps could be formulated, which under pulse compression could yield improved axial resolution and increase the −3 dB bandwidth of the imaging system. In that study, the frequency response of the source was assumed to be approximately Gaussian. An inverse Gaussian boost function (inverse of the frequency response) was used to create a pre-enhanced FM chirp that could be used under pulse compression to effectively increase the −3 dB bandwidth of the received signal. The pre-enhanced FM chirp was created by weighting a linear FM chirp function with the inverse of the approximate frequency response of the system. Pulse compression was accomplished by taking the autocorrelation of the measured waveforms (a matched filtering approach). The technique increased the −3 dB bandwidth of the source by 40–50%, but with some increase in the sidelobe levels. Another possible effect of using preenhanced chirps is the heating of the transducer because frequencies are being transmitted with higher amplification when the transducer is less efficient in converting voltage to ultrasound.

The purpose of the present study is to evaluate the use of pre-enhanced FM chirps to improve the axial resolution and effectively increase the −3 dB pulse/echo bandwidth and the useable bandwidth of the ultrasonic imaging system using a mismatched filtering scheme. A technique is developed to construct optimal pre-enhanced FM chirps. Furthermore, the new technique, called the resolution enhancement compression (REC) technique, enables the enhancement of axial resolution in the imaging system without large sidelobe levels. The −3 dB bandwidth is doubled using pre-enhanced chirps with minimal range sidelobes (experimentally determined to be less than 45 dB below the mainlobe). The REC technique offers four distinct novelties over the techniques introduced by Raman and Rao [16] and Venkatraman and Rao [17]. First, the pre-enhanced chirps are constructed using convolution equivalence and the impulse response of the actual source. In the context of the REC technique, convolution equivalence states that the impulse response of the source convolved with the pre-enhanced FM chirp is equal to the desired impulse response of larger bandwidth convolved with a simple linear FM chirp. Second, pulse compression is accomplished through mismatched filtering in the frequency domain as opposed to autocorrelation of the measured waveforms. Third, the REC technique makes use of convolution equivalence to decrease sidelobe levels over the approach by Raman and Rao. Finally, by using the convolution equivalence, the shape of the compressed waveform can be controlled better and to a limited degree shaped to the user's application. For example, Raman and Rao were able to increase the bandwidth by 50%, but the REC technique enables the bandwidth of the source to be doubled.

II. Theory

Consider an ultrasonic imaging system with shift-varying impulse response, $h(nT, \mathbf{x})$, that is used to measure the echo from a three-dimensional, random-scattering object, $f(\mathbf{x})$ with time sampled on the interval T with integer n. The nth echo sample, $g'[n]$, measured with the source is given by the continuous-to-discrete integral transformation [12]:

$$g'[n] = \int_{-\infty}^{\infty} h(nT, \mathbf{x}) f(\mathbf{x}) d^3x + e'[n], \tag{1}$$

where $e'[n]$ is a sample of the signal independent noise vector that is considered to be a wide-sense, stationary random process.

The total shift-varying response of the imaging system is the convolution of the impulse response of the source and the voltage waveform used to excite the source:

$$h(nT, \mathbf{x}) = \sum_{m=-\infty}^{\infty} v_1[n-m] h_1(mT, \mathbf{x}) = \{v_1 * h_1\}(mT, \mathbf{x}), \tag{2}$$

where $v_1[n]$ is the voltage waveform and $h_1(nT, \mathbf{x})$ is the pulse-echo impulse response of the system. The total shift-varying response is not unique to a particular pulse-echo impulse response of the system. Some pulse-echo impulse response may exist for an imaging system, $h_2(nT, \mathbf{x})$, that, when convolved with a different voltage waveform, $v_2[n]$, is equivalent to (2) or:

$$\{v_1 * h_1\}(mT, \mathbf{x}) = \{v_2 * h_2\}(mT, \mathbf{x}), \tag{3}$$

for some spatial location. Eq. (3) implies convolution equivalence between two different impulse responses convolved with the appropriate voltage waveforms. An example of convolution equivalence is illustrated in Fig. 1. Two different impulse response functions [Fig. 1(a) and (b)] are convolved with two FM chirps [Fig. 1(c) and (d)] to yield an equivalent convolved waveform [Fig. 1(e)].

Suppose that the voltage waveform used to excite the source with impulse response, $h_2(nT, \mathbf{x})$, is given by the linear FM chirp sequence:

$$\begin{aligned} v_2[n] &= v_{\text{Lin-chirp}}[n] \\ &= w[n] \exp\left\{ i2\pi \left(f_0 nT + \frac{\Delta f}{T_p} (nT)^2 \right) \right\}, \end{aligned} \tag{4}$$

where f_0 is the center frequency of the chirp, $\Delta f / T_p$ is the frequency-ramp constant in megahertz μs^{-1} and $w[n]$ is a Tukey window function [12] as shown in (5) (see next page), where N is the number of samples in the window

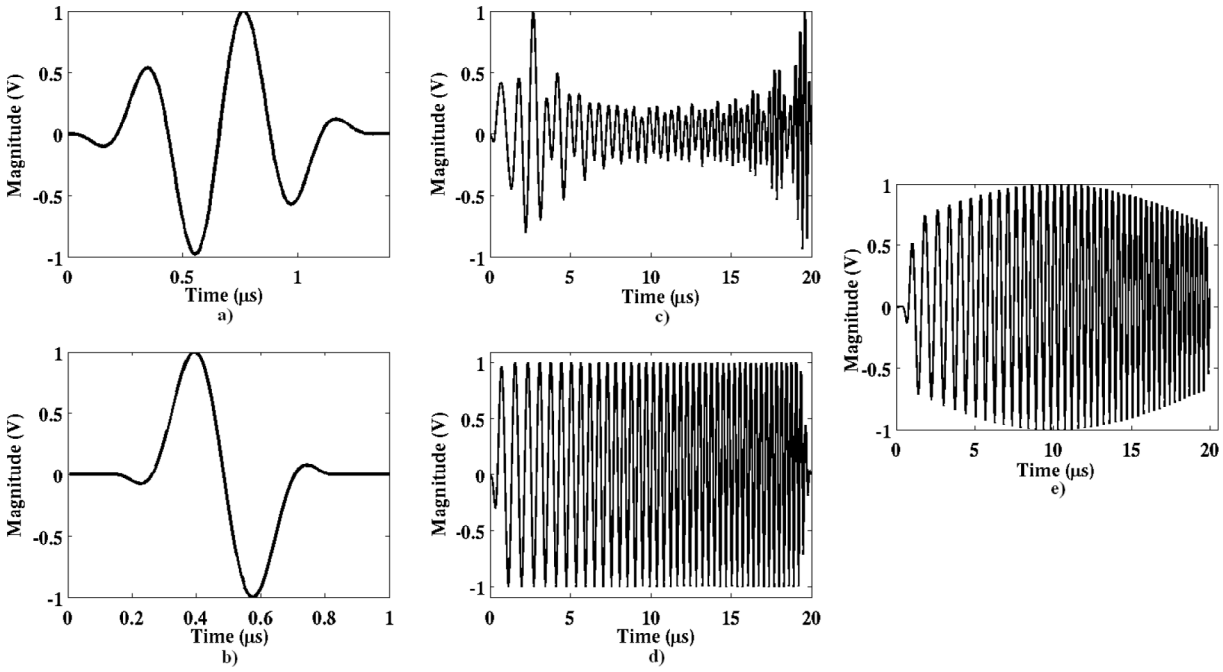

Fig. 1. Simulated impulse responses, chirps, and convolutions. (a) Pulse with approximately 48% −3 dB pulse/echo bandwidth. (b) Pulse with approximately 97% −3 dB pulse/echo bandwidth. (c) Modified chirp used to excite the 48% bandwidth source. (d) Linear chirp used to excite the 97% bandwidth source. (e) Convolution of the pulses with their respective chirps sequences.

$$w[n] = \begin{cases} 1.0, & 0 \le |n| \le \frac{N}{2}[1+\alpha], \\ 0.5\left[1.0 + \cos\left(\pi \frac{n - \frac{N}{2}[1+\alpha]}{N[1-\alpha]}\right)\right], & \frac{N}{2}[1+\alpha] \le |n| \le N, \end{cases} \tag{5}$$

and α determines the ratio of tapering to constant window size ($\alpha = 0, 1$ represents rectangular and Hanning windows, respectively). If a different FM chirp sequence (we denote as the pre-enhanced FM chirp or $v_{\text{P-chirp}}[n]$) is used to excite the source with impulse response, $h_1(nT, \mathbf{x})$, such that:

$$\begin{aligned} v_1[n] &= v_{\text{P-chirp}}[n] \\ &= w[n] \exp\left\{ i2\pi \left(f_0 nT + \frac{\Delta f}{T_p}(nT)^2 \right) \right\} * \psi[n] \\ &= v_{\text{Lin-chirp}}[n] * \psi[n], \end{aligned} \tag{6}$$

then $\psi[n]$ is some undetermined function that can be found through application of convolution equivalence. From (3):

$$v_{\text{P-chirp}}[n] * h_1(nT, x) = v_{\text{Lin-chirp}}[n] * h_2(nT, x). \tag{7}$$

In frequency domain:

$$V_{\text{P-chirp}}(u) \times H_1(u, \mathbf{x}) = V_{\text{Lin-chirp}}(u) \times H_2(u, \mathbf{x}), \tag{8}$$

where u is the discrete frequency sampling variable. Rearranging the terms yields:

$$\begin{aligned} V_{\text{P-chirp}}(u) &= V_{\text{Lin-chirp}}(u) \times \frac{H_2(u, \mathbf{x})}{H_1(u, \mathbf{x})} \\ &= V_{\text{Lin-chirp}}(u) \times \psi(u, \mathbf{x}), \end{aligned} \tag{9}$$

where $\psi(u, \mathbf{x}) = H_2(u, \mathbf{x}) / H_1(u, \mathbf{x})$.

Now suppose that $h_1(nT, \mathbf{x})$ represents the pulse-echo impulse response of a weakly-focused transducer with −3 dB pulse/echo bandwidth of 50% that is excited with the voltage waveform, $v_{\text{P-chirp}}[n]$. Pulse compression of the coded waveforms is achieved by using appropriate filters to minimize the correlation length of the received echo signals. However, because of convolution equivalence, it also is possible to choose filters that will reduce the correlation length of the received echo signals so that they are approximately equal to some alternate impulse response, $h_2(nT, \mathbf{x})$. $h_2(nT, \mathbf{x})$ can be artificially created to have properties that may be useful to the imaging system, e.g., a −3 dB bandwidth of 100%. Pulse compression is achieved through:

$$g[n] = \sum_{m=-\infty}^{\infty} b[m-n] g'[m], \tag{10}$$

where $b[n]$ is some filtering function. If $b[n]$ is chosen such that $b[n] = v^{-1}_{\text{Lin-chirp}}[n]$ then (10) becomes:

$$g[n] = \sum_{m=-\infty}^{\infty} v^{-1}_{\text{Lin-chirp}}[m-n]g'[m] \qquad (11)$$
$$= \sum_{m=-\infty}^{\infty} v^{-1}_{\text{Lin-chirp}}[m-n]\int_{-\infty}^{\infty} h(mT,\mathbf{x})f(\mathbf{x})d^3x + e[n],$$

where $e[n]$ is the filtered noise. The convolution equivalence of (3) and the definition of the total response of the system in (2) gives:

$$g[n] = \sum_{m=-\infty}^{\infty} v^{-1}_{\text{Lin-chirp}}[m-n] \times \int_{-\infty}^{\infty} \sum_{l=-\infty}^{\infty} v_{\text{P-chirp}}[m-l]h_1(lT,\mathbf{x})f(\mathbf{x})d^3x + e[n],$$
$$g[n] = \sum_{m=-\infty}^{\infty} v^{-1}_{\text{Lin-chirp}}[m-n] \times \int_{-\infty}^{\infty} \sum_{l=-\infty}^{\infty} v_{\text{Lin-chirp}}[m-l]h_2(lT,\mathbf{x})f(\mathbf{x})d^3x + e[n], \qquad (12)$$
$$g[n] = \sum_{l=-\infty}^{\infty} K\delta[l-n]\int_{-\infty}^{\infty} h_2(lT,\mathbf{x})f(\mathbf{x})d^3x + e[n],$$

where K is the TBP of $v_{\text{Lin-chirp}}[n]$.

Examination of (12) yields two important results of pulse compression and the use of the convolution equivalence. The compressed echo sequence depends on the interaction of $h_2(nT,\mathbf{x})$ with the scattering object, $f(x)$, as opposed to actual impulse response of the system, $h_1(nT,\mathbf{x})$. As a result, the axial resolution of the imaging system is improved over conventional pulse-echo techniques because the -3 dB pulse-echo bandwidth (Gaussian bandwidth) of $h_2(nT,\mathbf{x})$ was constructed to be larger than the bandwidth of $h_1(nT,\mathbf{x})$. The REC technique is defined by using convolution equivalence to create a pre-enhanced chirp and the filtering scheme used in (10) to improve the axial resolution of the imaging system.

The second result revealed by examination of (12) is that the eSNR of the compressed waveform is increased by a factor related to the TBP of $v_{\text{Lin-chirp}}[n]$ compared to the uncompressed echo waveform. The eSNR is defined as [12]:

$$\text{eSNR}[n] = 10\log\left(\frac{\mathsf{E}\left\{\left|K\int_{-\infty}^{\infty} h_2(nT,\mathbf{x})f(\mathbf{x})d^3x\right|^2\right\}}{\mathsf{E}\left\{|e[n]|^2\right\}}\right)$$
$$= 10\log\left(\frac{K^2\sigma_f^2}{K\sigma_e^2}\int_{-\infty}^{\infty} h_2^2(nT,\mathbf{x})d^3x\right) \qquad (13)$$
$$= 10\log K + \text{eSNR}'[n],$$

where σ_f^2 and σ_e^2 are the object and noise variances, E represents the expectation value, and eSNR$'$ is the echo-signal-to-noise ratio for the conventional pulsing scheme. Eq. (13) indicates that the increase in eSNR for the pulse compression is larger than the eSNR$'$ by $10\log K = 10\log\text{TBP}$. One other effect of the filtering process is that the noise will not be zero-mean, white Gaussian noise (WGN) because certain frequency components in the noise spectrum will be amplified by the filters more than other frequency components.

III. Experimental Implementation

A. Overview

To validate the theoretical predictions, a set of simulations were constructed, and experimental measurements were taken. The simulations and experiments made use of the REC technique to increase the -3 dB pulse/echo bandwidth of the imaging system and improve its axial resolution. Useable bandwidth, gain in eSNR, sidelobe levels, effects of noise, and processing strategies also were examined.

B. Quality Metrics

To evaluate the improvement in axial resolution, and therefore image quality using the REC technique in ultrasonic imaging, the following quality metrics were used.

1. eSNR: The eSNR of waveforms resulting from pulse compression is improved over conventional pulsing techniques. Pulse compression increases the echo signal energy more than the noise signal. The gain in eSNR results from the increase in the TBP of the voltage waveforms used to excite the source. The eSNR of echo waveforms arising from scatterers in the ultrasonic field can be estimated through (13). In the frequency domain, $\overline{\text{eSNR}}$ describes the average eSNR per frequency channel and is defined as:

$$\overline{\text{eSNR}}(u|\mathbf{x}) = \frac{|H_{2c}|\,(u|\mathbf{x})^2\,\mathsf{E}\left\{|F(u)|^2\right\}_f}{\mathsf{E}\left\{|E(u)|^2\right\}_e}, \qquad (14)$$

where $|E(u)|^2$ is the power spectral density of the noise, and $H_{2c}(u|\mathbf{x})$, $F(u)$ represent the Fourier transforms of $h_{2c}(nT,\mathbf{x})$, $f(x)$, respectively [18]. $h_{2c}(nT,\mathbf{x})$ is the ensemble average of the compressed signal over noise:

$$h_{2c}(nT,\mathbf{x}) = \mathsf{E}\left\{g[n]\right\}_{\text{noise}}. \qquad (15)$$

2. Bandwidth: An important metric in determining the ability of the REC technique to provide improvements in axial resolution is the bandwidth. Furthermore, in QUS imaging, increased bandwidth reduces the variance of scatterer size estimates [14], [15]. Typically, a Gaussian spectrum is assumed for the source power spectrum, and the bandwidth is defined as the width of the Gaussian function in which the magnitude falls by one-half (the -3 dB pulse/echo bandwidth). If the source power spectrum is Gaussian, then the -3 dB pulse/echo bandwidth is important because it reflects the axial resolution of the imaging

system, i.e., a larger −3 dB pulse/echo bandwidth yields an improved axial resolution.

The limitation of defining bandwidth in terms of the −3 dB bandwidth is that the useable bandwidth is not defined. Useable bandwidth will be determined by the amplitude of the signal relative to the noise floor. For the purposes of QUS imaging, we define the useable bandwidth as the portion of the power spectrum 6 dB above the noise or the +6 dB $\overline{\text{eSNR}}$. The useable bandwidth will change, depending on the backscattering strength of the object and the attenuation of the medium. In some instances, the useable bandwidth may be larger than the −3 dB pulse/echo bandwidth, and in other instances less.

3. Modulation Transfer Function: To measure the axial resolution of an imaging system, the MTF is a common metric. The MTF is superior to bandwidth in representing the resolution of a system. A chirp can have longer duration than a short pulse, but it could have the same −3 dB bandwidth. The MTF curve will fall more rapidly for the longer duration chirp than the shorter pulse. The MTF describes the ability of the imaging system to transfer object contrast to the image. The MTF represents the spatial frequencies that are passed by the imaging system. The MTF is defined as [19]:

$$\text{MTF}(k|\mathbf{x}) = \frac{|H(k|\mathbf{x})|}{|H(0|\mathbf{x})|}, \tag{16}$$

where $|H(k|\mathbf{x})|$ represents the magnitude of the spatial Fourier transform of the envelope of the echo waveform. The axial resolution can be quantified by determining the wavenumber, k, to which the MTF falls to 0.1. A larger k value corresponds to a better axial resolution for the imaging system. The axial resolution of the imaging system can be defined as:

$$\lambda_{\text{res}} = \frac{1}{2}\frac{2\pi}{k_0}\ (\text{m}), \tag{17}$$

where k_0 is the value of k at which the MTF falls to 0.1.

C. Simulation

The goal of the simulations is to validate the theory and to guide the experimental measurements. The impulse response at the focus of a single-element, weakly-focused transducer was simulated. The center frequency of the impulse response was 2.25 MHz. The impulse response for the simulated source at the focus (∼48% −3dB bandwidth) and the desired impulse response (∼97% −3dB bandwidth) are displayed in Fig. 1(a) and (b). A linear FM chirp [Fig. 1(d)] was convolved with the 97% bandwidth impulse response. The linear FM chirp was tapered with a Tukey-cosine window from (5) with an 8% taper and had a duration of 20 μs. The tapering was introduced to reduce the effects of sidelobes [9]. From the convolved excitation waveform, (9) was used to find a pre-enhanced FM chirp that would be used to excite the simulated 48% bandwidth source, except that the filter, $\psi(u, \mathbf{x})$, was replaced with a Wiener filter:

$$\psi_{\text{sim}}(u|\mathbf{x}) = \frac{H_1^*(u|\mathbf{x})}{|H_1(u|\mathbf{x})|^2 + |H_1(u|\mathbf{x})|^{-2}}. \tag{18}$$

In general, $\psi_{\text{sim}}(u|\mathbf{x})$ is a spatially varying function because the impulse response is a spatially varying function. However, in simulations and subsequent experimental implementation, the impulse response was considered to be spatially nonvarying over the depth-of-focus of the source and, therefore, $\psi_{\text{sim}}(u|\mathbf{x})$ also was assumed to be spatially nonvarying over the depth-of-focus. The resulting pre-enhanced FM chirp was weighted with a Tukey-cosine window with an 8% taper. The tapering was applied to reduce side-lobe levels. The pre-enhanced FM chirp is displayed in Fig. 1(c).

The pre-enhanced FM chirp was used to excite the simulated 48% bandwidth source, and the waveform was reflected from a planar surface located at the focus surrounded by water. The waveform reflected from the planar surface was compressed using a frequency domain representation of (10):

$$G(u) = \beta_{\text{REC}}(u)G'(u), \tag{19}$$

where $\beta_{\text{REC}}(u)$ is the compression filter (a Wiener filter):

$$\beta_{\text{REC}}(u) = \frac{V'^*_{\text{Lin-chirp}}(u)}{\left|V'_{\text{Lin-chirp}}(u)\right|^2 + \gamma\overline{\text{eSNR}}^{-1}(u)}, \tag{20}$$

with $\gamma = 1$. The compressed waveform is obtained by taking the inverse Fourier transform of (19). The choice γ allows the trade-off between axial resolution, gain in eSNR, and sidelobe levels. Typically, smaller values of γ lead to better axial resolution and sidelobes but less gain in eSNR (an inverse filter response). The optimal setting for γ will depend on the level of noise and desired axial resolution. Large values of γ cause the Wiener filter to approach a matched filter response, which reduces the axial resolution but gives the maximum increase in eSNR.

$V'_{\text{Lin-chirp}}(u)$ is the frequency domain representation of a modified linear FM chirp. The modified linear FM chirp is similar to the linear FM chirp used to find the pre-enhanced FM chirp in (9). By tapering the pre-enhanced FM chirp, the convolution equivalence no longer holds with the original linear FM chirp from (9). Therefore, using a compression filter with the original linear FM chirp would yield increased sidelobes. To obtain an improved performance, a modified linear FM chirp was obtained through:

$$V'_{\text{Lin-chirp}}(u) = V_{\text{P-chirp}}(u) \times \frac{H_1(u, \mathbf{x})}{H_2(u, \mathbf{x})}. \tag{21}$$

Use of the modified linear FM chirp in the compression filter gave sidelobes that were 15 dB below sidelobes occurring with use of the original FM linear chirp. Therefore, in both simulations and experiments, a modified linear FM chirp was estimated and used in the compression filters.

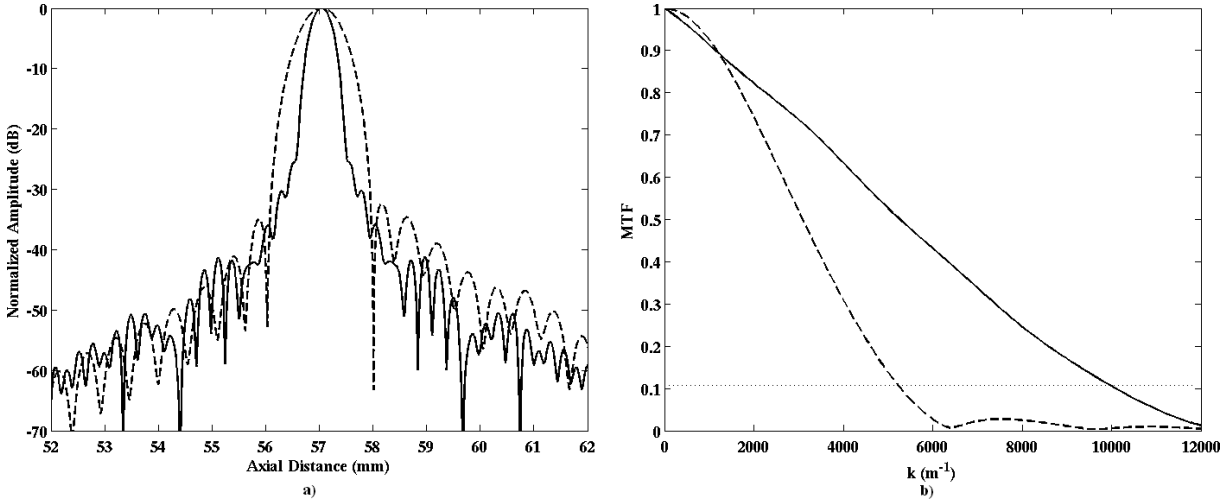

Fig. 2. (a) Envelope of compressed waveforms. (b) MTF curve of the two compressed waveforms (--, elementary pulse compression technique; —, the REC technique).

A linear FM chirp also was used to excite the simulated 48% bandwidth source. The linear FM chirp used to excite the simulated source was 20 μs in length, had a bandwidth that was 1.14 times the −3 dB pulse/echo bandwidth of the source, and had an 8% taper. The resulting waveform reflected from the planar surface was compressed using a Wiener filter (20) based on the linear FM chirp (we denote here as the elementary pulse compression technique) in order to compare the performance of the REC technique with elementary pulse compression techniques.

The envelopes of each of the two compressed waveforms reflected from the planar surface are displayed in Fig. 2(a). Examination of Fig. 2(a) reveals that the width of the mainlobe is smaller for the waveform that was excited with the pre-enhanced FM chirp and compressed with the REC technique. The smaller mainlobe translates into improved axial resolution using the REC technique. The sidelobe levels are smaller for the elementary pulse compression techniques versus the REC technique. However, the sidelobe levels still are more than 40 dB below the mainlobe levels using the REC technique. Although they have yet to be tried in the context of the REC technique, other techniques can be tested to further reduce these sidelobe levels (typically at the cost of some spatial resolution) [6], [11], [20], [21]. The MTF curve [Fig. 2(b)] indicates that the axial resolution using the REC technique was improved. The k-value at which the MTF curve falls to 0.1 occurs at 10,090 and 5279 m^{-1} (λ_{res} values of 0.29 mm and 0.60 mm) for the REC technique and elementary pulse compression technique, respectively.

The bandwidth of the compressed waveform can be determined by considering the −3 dB pulse/echo bandwidth [Fig. 3(a)] and the useable bandwidth [Fig. 3(b)]. The power spectra of the compressed waveforms using the REC technique and elementary pulse compression are displayed in Fig. 3(a). Examination of the pre-enhanced FM chirp reveals that more energy is being excited in frequencies farther away from the center frequency of the impulse response. Because frequencies on the bandwidth edges are excited with greater energy, the compressed waveform can have a broadened bandwidth. The −3 dB pulse/echo bandwidths of the impulse response of the source and the compressed waveform using the pre-enhanced FM chirp and the REC technique are 1.08 MHz (48%) and 2.18 MHz (97%), respectively. Use of the REC technique approximately doubled the −3 dB bandwidth of the imaging system over the impulse response of the source.

The useable bandwidth is defined from the noise floor, +6 dB $\overline{\mathrm{eSNR}}$, and it describes the frequency channels that are useable for QUS estimates. Fig. 3(b) displays the useable bandwidths of the simulated waveforms compressed with the REC technique and the elementary pulsing technique. Zero-mean WGN was added to the excited waveforms such that the uncompressed waveform and the pulsed waveform had an eSNR value of approximately 14 dB. Examination of Fig. 3(b) reveals that the useable bandwidth from the REC technique is significantly larger than the useable bandwidth from pulsing techniques (2.7 MHz as opposed to 1.7 MHz). Fig. 3(b) reveals how the REC technique redistributes energy into frequency channels further from the center frequency of the impulse response by increasing the energy in these frequency channels on transmit.

D. Experimental Setup

The theoretical predictions also were validated through a series of experimental measurements. A single-element, weakly-focused (f/3) transducer (Panametrics; Waltham, MA) was used in the experimental measurements. The transducer had a center frequency of 2.25 MHz and a 56% −3 dB pulse/echo bandwidth. Fig. 4(a) is an image of the impulse response voltage measured from the reflection off of a planar surface surrounded by water at room temperature.

Chirp waveforms were excited with an arbitrary waveform generator (Lecroy LW 400A, Chestnut Ridge, NY)

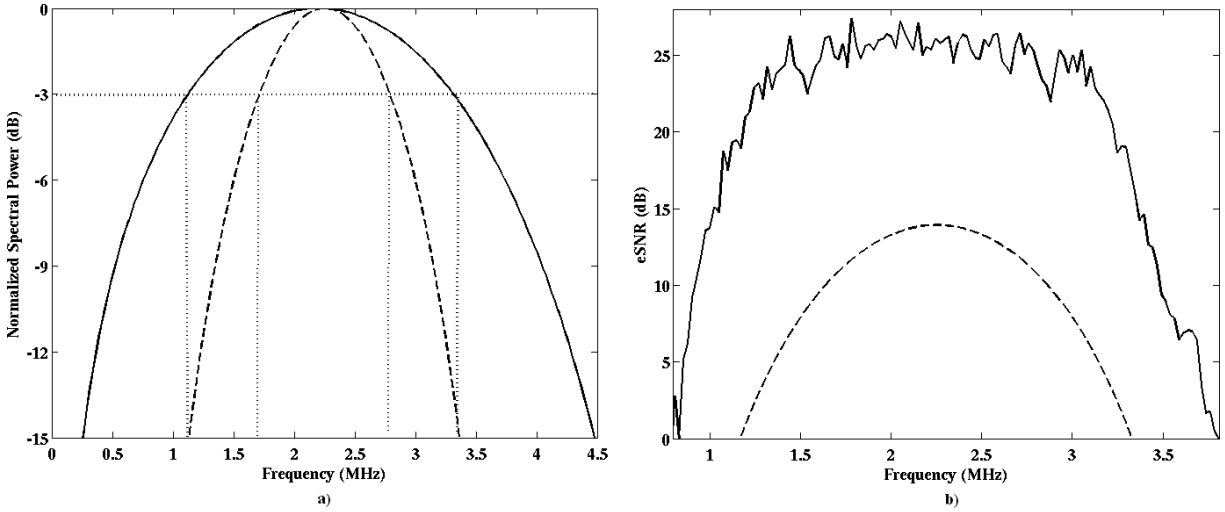

Fig. 3. (a) Power spectra. (b) $\overline{\text{eSNR}}$ curves for waveforms reflected from a planar surface (--, conventional pulsing technique; —, the REC technique).

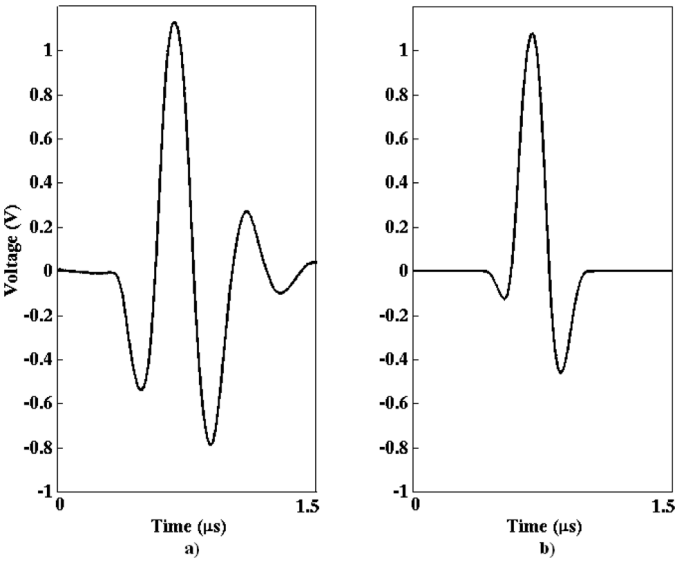

Fig. 4. (a) Impulse response of the transducer. (b) Pulse constructed with double the −3 dB pulse/echo bandwidth of the impulse response of the transducer.

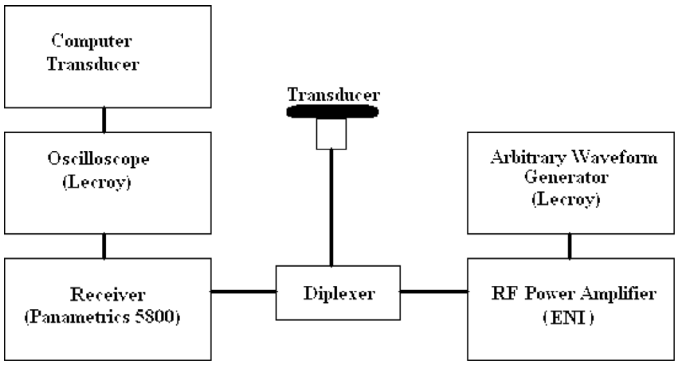

Fig. 5. Diagram of the experimental setup.

with a sampling frequency of 400 MHz. The chirp signals were created with Matlab (The Mathworks Inc., Natick, MA) and downloaded to the arbitrary waveform generator. The signal was amplified with a 2100L RF power amplifier (ENI, Rochester, NY). The amplified signal (50 dB) was connected to the transducer through a diplexer. The received echo signal was connected to a Panametrics 5800 (Waltham, MA), which in turn was connected to an oscilloscope (Lecroy 9354 TM, Chestnut Ridge, NY). Fig. 5 is a diagram of the experimental setup.

Three sets of experiments were conducted to examine the pulse compression technique and assess the ability to improve axial resolution and bandwidth. The first experiment consisted of measurements from a Plexiglas® reflector located at the focus of the transducer. The second experiment consisted of taking measurements from a tungsten wire of 250-μm diameter. The third experiment consisted of taking measurements from a series of 4 tungsten wires of 250-μm diameter spaced approximately at 0.535, 0.535, and 0.355 mm apart. All measurements were conducted in a tank of degassed water at room temperature.

E. Implementation of Compression Algorithms

The impulse response of the transducer was measured from a planar Plexiglas® reflector located at the focus of the transducer [Fig. 4(a)] excited with the Panametrics 5800 pulser/receiver. A new impulse response function with double the bandwidth of the actual impulse response of the source was constructed by placing a Hanning window half the length of the impulse response of the source at the center of the gated impulse response [Fig. 4(b)]. The impulse responses are described by the functions $h_1(nT, \mathbf{x})$ and $h_2(nT, \mathbf{x})$, respectively.

The new pulse of larger bandwidth, $h_2(nT, \mathbf{x})$, was convolved with a linear FM chirp, $v_{\text{Lin-chirp}}[n]$. The −3 dB bandwidth of $v_{\text{Lin-chirp}}[n]$ was approximately 1.14 times the −3 dB pulse/echo bandwidth of $h_2(nT, \mathbf{x})$ in order to minimize sidelobe levels [20]. In addition, $v_{\text{Lin-chirp}}[n]$ was weighted with a Tukey-cosine window with an 8% taper

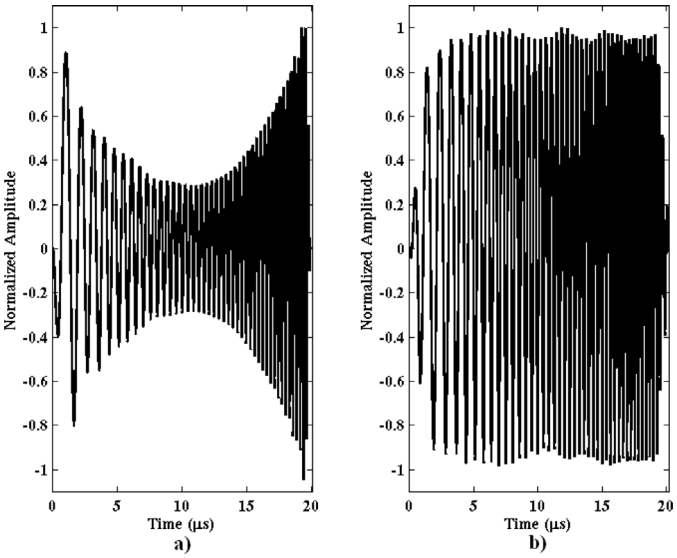

Fig. 6. (a) Pre-enhanced FM chirp used to excite the transducer. (b) The linear FM chirp used in the REC technique.

to further reduce sidelobe levels. The linear FM chirp was 20 μs in duration. Eq. (9) and (18) were used to find a pre-enhanced FM chirp that would be used to excite the transducer, except the actual transfer function of the transducer was used instead of the simulated source. The resulting pre-enhanced FM chirp was tapered with a Tukey-cosine window with an 8% taper. The tapering was applied to reduce sidelobe levels in the subsequent pulse compression. The pre-enhanced FM chirp is displayed in Fig. 6(a).

By tapering the pre-enhanced FM chirp, the convolution equivalence no longer holds. To reestablish convolution equivalence, a modified linear FM chirp was calculated as in the simulations. The transducer was excited using the pre-enhanced FM chirp. The resultant waveforms were measured with the same transducer (pulse/echo) and recorded from the oscilloscope for postprocessing. The waveform was initially measured from a planar Plexiglas® reflector located at focus of the transducer oriented normal to the propagation axis. The measured waveform then was filtered (not compressed) according to (21) to find $v'_{\text{Lin-chirp}}[n]$, which was used in the subsequent compression algorithms. The TBP of $v'_{\text{Lin-chirp}}[n]$ was calculated at 49.0, yielding a maximum predicted increase in eSNR of 16.9 dB.

Implementation of the REC technique consisted of constructing the pre-enhanced FM chirp, recording the measured RF signal (from the impulse response of the transducer excited with the pre-enhanced FM chirp) from some scattering object, constructing the appropriate filter, and filtering the signal according to (20). In the experimental measurements, the REC technique filter was given by the Wiener filter:

$$\beta_{\text{REC}}(u) = \frac{V'^{*}_{\text{Lin-chirp}}(u)}{\left|V'_{\text{Lin-chirp}}(u)\right|^2 + \gamma\overline{\text{eSNR}}^{-1}(u|\mathbf{x})} \quad (22)$$

with $\gamma = 1$ for most of the experiments.

F. Addition of Noise

The effects of noise on image quality using the REC technique were examined by adding zero-mean WGN to the measured data. The eSNR was quantified from the measured data at a particular spatial location through (13). For this study, it was desired to examine data with four different values of eSNR (the actual eSNR of the measured data (∼37 dB) and eSNR values of 15, 9, and 3 dB). To examine the data with eSNR values smaller than the actual measured values, zero-mean WGN was added to the acquired data. The variance of the zero-mean WGN added to the measured RF signal was determined from the sample variance measured from the data and the desired eSNR level.

IV. Experimental Results

The pre-enhanced FM chirp used to excite the transducer and the modified linear FM chirp used in the pulse compression algorithms are displayed in Fig. 6. In the first set of experiments, pre-enhanced FM chirps and the REC technique were used to examine the axial resolution enhancement from reflections off of a planar reflector. The transducer was excited with the pre-enhanced FM chirp, and the resultant waveform was reflected from a Plexiglas® plate located at the focus of the transducer oriented normal to the axis of propagation.

The graphs of Fig. 7 indicate that the improvement in axial resolution due to the REC technique was significant. The graphs of the envelopes of the reflected signal are displayed in Fig. 7(a). The width of the envelope at −6 dB is almost two times smaller using the REC technique over conventional pulsing techniques (the impulse response of the source). Comparison of the REC technique and conventional pulsing techniques [Fig. 7(b)] reveal that the REC technique outperformed the conventional pulsing technique in terms of axial resolution as defined from the MTF. The MTF value at which k-value fell to 0.1 corresponded to 10,300 and 7500 m^{-1} for the REC technique and conventional pulsing technique, respectively. The MTF values corresponded to axial resolutions of 0.305 and 0.420 mm, respectively.

Another important consideration in using the REC technique is to quantify the subsequent −3 dB pulse/echo bandwidth and the $\overline{\text{eSNR}}$ of the compressed waveform. Fig. 8 displays the −3 dB pulse/echo bandwidth and the $\overline{\text{eSNR}}$ of the compressed waveform from reflections off a planar reflector located at the focus. The −3 dB pulse/echo bandwidth of the waveform compressed using the REC technique [Fig. 8(a)] was 113% and more than double that of the system impulse response (56%). The measured impulse response of the system and the uncompressed waveform had an eSNR of 37 dB achieved by adding zero-mean WGN to the waveforms.

Two important features are revealed from Fig. 8(b). First, over the −3 dB pulse/echo bandwidth, the com-

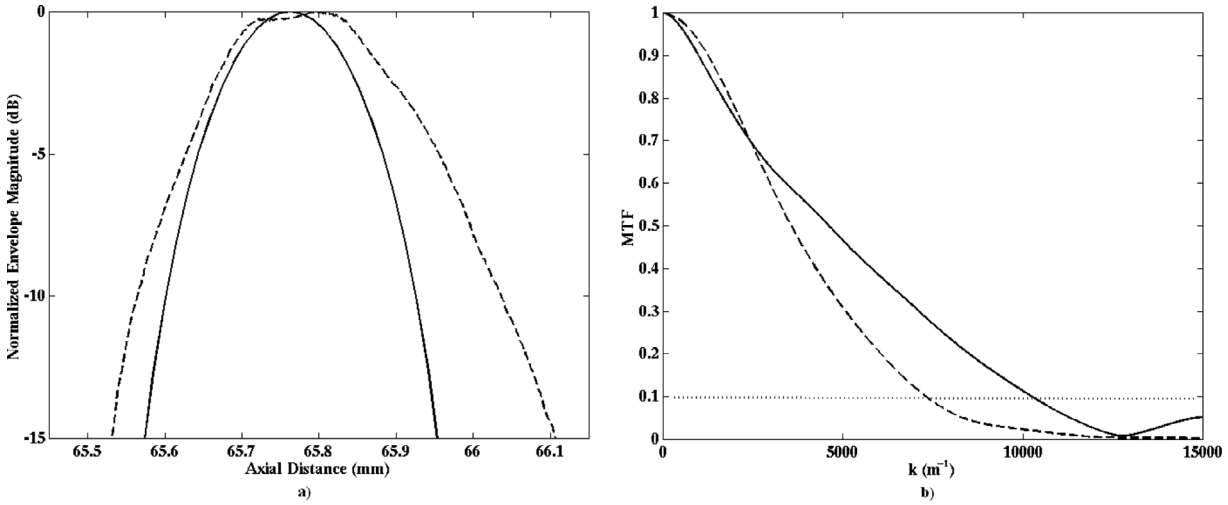

Fig. 7. (a) Envelopes of waveforms reflected from planar reflector located at focus. (b) The MTF curves of the resulting waveforms (--, conventional pulsing technique; —, the REC technique).

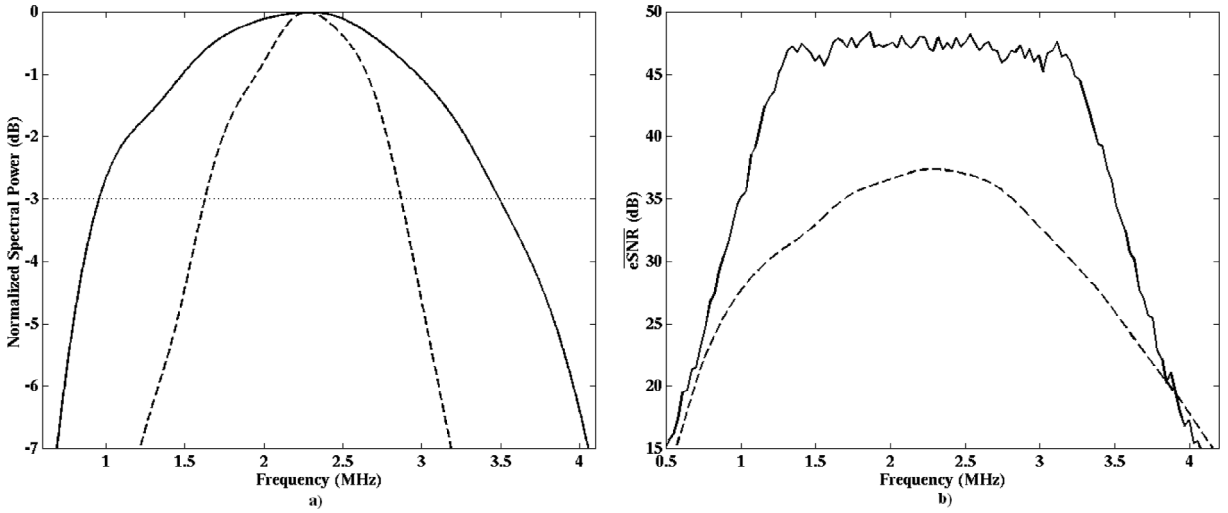

Fig. 8. (a) Power spectra of the measured waveforms from the planar reflector. (b) The resulting $\overline{\text{eSNR}}$ of the measured waveforms (--, conventional pulsing technique; —, the REC technique).

pressed waveform using the REC technique had significantly larger $\overline{\text{eSNR}}$ compared to the waveform measured using the conventional pulsing technique (gain in eSNR was approximately 11 dB). Second, the gain in $\overline{\text{eSNR}}$ was observed to be larger for those frequency bands in which more energy was excited with the pre-enhanced chirp. The boost in energy at these frequency bands comes from the transmitted chirp sequence. A sharp fall-off in $\overline{\text{eSNR}}$ occurs at those frequency bands in which no excitation energy in the chirp was transmitted to the transducer (< 0.5 MHz and > 4.0 MHz); and, as a result, on compression those frequency bands can yield lower $\overline{\text{eSNR}}$ values than comparable frequencies using the conventional pulsing technique. The sharp fall-off in $\overline{\text{eSNR}}$ is a source of sidelobes under pulse compression.

The actual compressed pulse is plotted in Fig. 9(a). Comparison of the actual compressed pulse using the REC technique and the desired pulse from Fig. 4(b) reveals minimal differences. Sidelobe levels using the REC technique can be observed in Fig. 9(b). Using the REC technique, long-range sidelobes can be observed at about 6 mm out from the mainlobe (at 60 and 72 mm from the source). These long-range sidelobe are approximately 45 dB below the mainlobe levels. These sidelobe levels are comparable to what was achieved with conventional pulse compression using linear FM chirps of the same bandwidth.

The second set of measurements was the backscatter from a single tungsten wire located at the focus. Graphs of the envelope and MTF curves from the wire with conventional pulsing techniques and with the REC technique are displayed in Fig. 10. Both the graphs of the envelopes and the MTF curves indicate the axial resolution of imaging system was improved with the REC technique. The k-values at which the MTF curves fell to 0.1 occurred at values corresponding to axial resolution values of 0.440 and 0.310 mm for the conventional pulsing technique and the

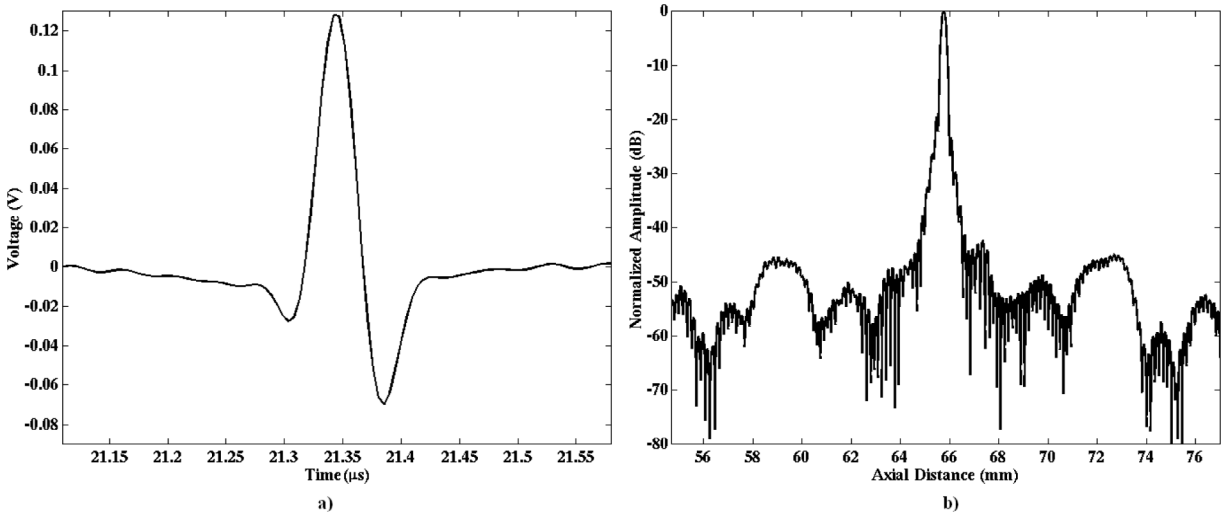

Fig. 9. (a) REC compressed pulse with double the −3 dB pulse/echo bandwidth of the impulse response of the transducer measured from reflection off of planar surface. (b) Envelope of the compressed waveform using the REC technique and the range sidelobes (∼45 dB below the mainlobe) located at 6 mm away from the mainlobe (60 and 72 mm).

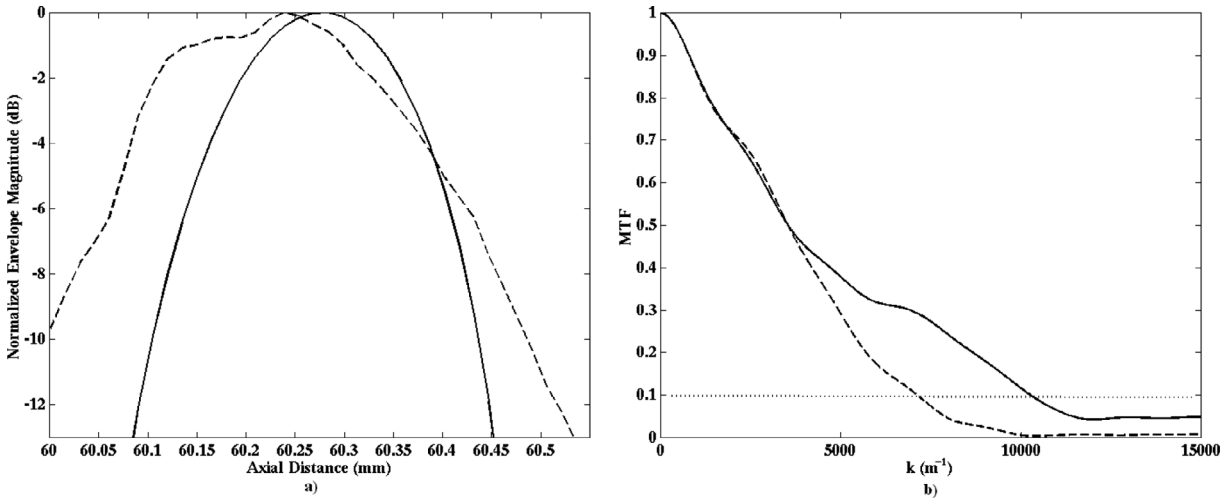

Fig. 10. (a) Envelopes of waveforms reflected from tungsten wire located at focus. (b) The MTF curves of the resulting waveforms (--, conventional pulsing technique; —, the REC technique).

REC technique, respectively. These axial resolution values will be important to understanding the final set of experiments conducted on a series of four tungsten wires spaced apart at different intervals.

The final set of experimental measurements was taken from a series of four tungsten wires. The wires were spaced at 0.535, 0.535, and 0.355 mm apart. According to the axial resolution predicted by the MTF curves for a single tungsten wire, the conventional pulsing technique should not be able to resolve the last two wires, but the REC technique should be able to resolve the last two wires. Fig. 11 shows B-modes images of the four wires after compression with both conventional pulsing techniques and with the REC technique. The B-mode image [Fig. 11(b)] from the REC technique reveals that the final two wires could be resolved. Use of conventional pulsing techniques did not allow the last two wires to be resolved [Fig. 11(a)].

The enhancement in the axial resolution is even more apparent in the Fig. 12. The actual waveform using the pre-enhanced chirp measured from the wires is displayed in Fig. 12(a). From the waveform using the pre-enhanced chirp, the number of wires and their relative locations cannot be resolved. After compression, the plot of the envelope [Fig. 12(b)] reveals that all four wires are resolved using the REC technique. However, in the envelopes using conventional pulsing, the last two wires cannot be resolved. Range sidelobes were assumed to be below the noise (eSNR of ∼37 dB in the compressed waveform) because they were nonapparent in the envelope images.

All of the measurements had large eSNR values (> 37 dB). The effects of reduced eSNR were examined by artificially adding zero-mean WGN to the measured RF data. The eSNR values examined were 3, 9, and 15 dB. Fig. 13 is a plot of the envelopes of the pulse reflected from

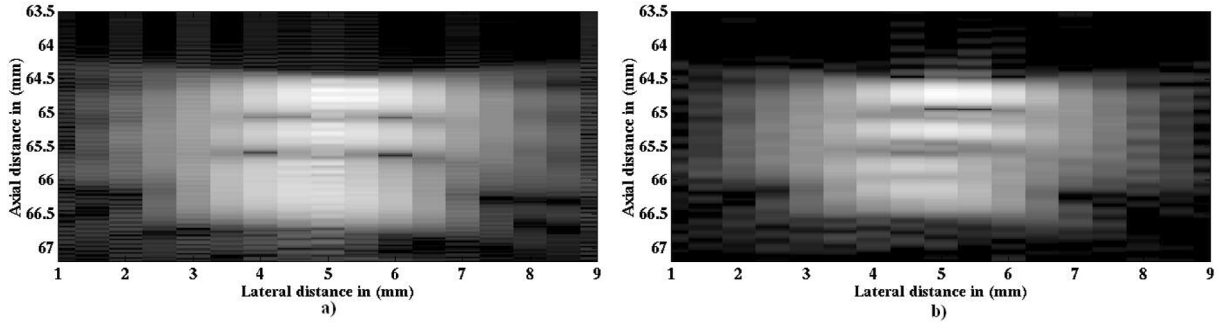

Fig. 11. B-mode images of four tungsten wires with (a) impulse response of transducer and (b) from the compressed waveforms using the REC technique. B-mode images have contrast of 50 dB.

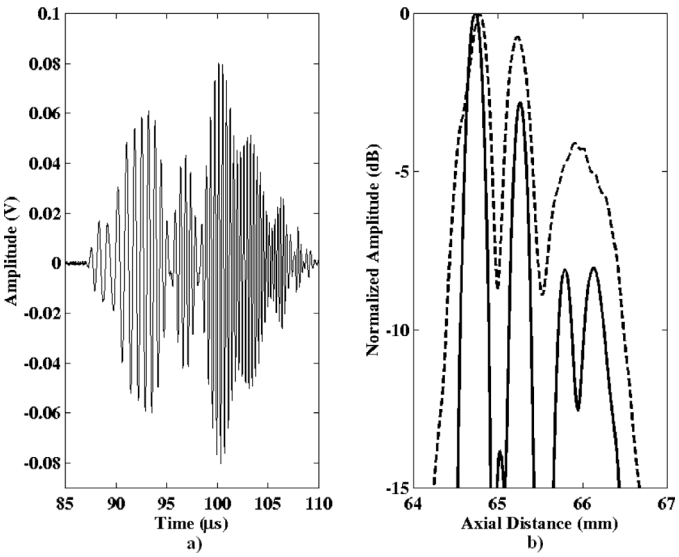

Fig. 12. (a) Uncompressed waveform measured from four tungsten wires. (b) The envelopes of the compressed waveform (--, conventional pulsing technique; —, the REC technique).

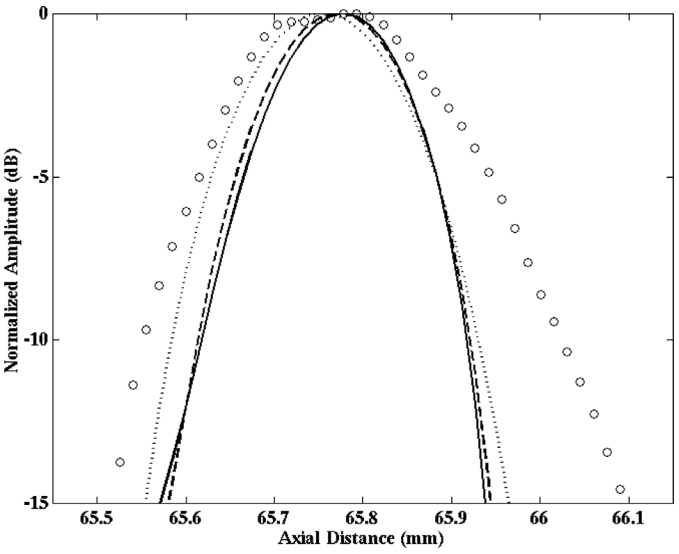

Fig. 13. Comparison of envelopes of impulse response, ○, with the compressed waveforms using the REC technique having eSNR values of 15 dB —, 9 dB --, 3 dB ⋯, reflected from a planar surface located at focus of the transducer.

the Plexiglas® plate after compression with the REC technique and a conventional pulsing technique. As the eSNR was decreased, the axial resolution of the compressed waveforms using the REC technique was reduced. However, the axial resolution of the compressed pulses using the REC technique continued to be dramatically improved over the conventional pulsing techniques for smaller eSNR values. In addition, the envelope curves reveal that the compressed waveforms using the REC technique gave a significant gain in the eSNR. The eSNR values of the compressed waveforms using the REC technique were quantified using (13). The new eSNR values were 24.2, 22.5, and 19.2 dB from the uncompressed eSNR values of 15, 9, and 3 dB, respectively. The boost in eSNR using the REC technique was 9.2, 13.5, and 16.2 dB from the 15, 9, and 3 dB uncompressed eSNR values, respectively.

The measurements from the four wires also were used to examine the effects of smaller eSNR on the ability to enhance the axial resolution of the compressed waveforms. Figs. 14(a)–(c) show graphs of the RF waveforms after adding in zero-mean WGN yielding eSNR values of 15, 9, and 3 dB, respectively. The resulting envelopes from the waveforms after compression using the REC technique also are shown in Fig. 14. The γ parameter was set at unity for all of these experiments, except for the uncompressed waveform with eSNR of 3 dB. The γ parameter was set to three in the lowest eSNR case because this was the value at which the last two wires were resolved when examining over several noise realizations. When the γ parameter was set lower than three in the low-noise case, examination of the compressed waveforms over several noise realizations did not consistently resolve the last two wires, i.e., in some noise realizations resolving the last two wires was masked by noise. The envelopes reveal that the enhancement in axial resolution remains significant, even in low eSNR conditions, and a significant gain in eSNR is achieved.

One of the main reasons for pursuing pulse compression techniques is the boost in eSNR achievable without increased pressure values. The boost in eSNR is achieved through increasing the TBP. Not only was the axial resolution enhanced through the REC technique, but a significant boost in the eSNR after compression also was observed in Figs. 13 and 14.

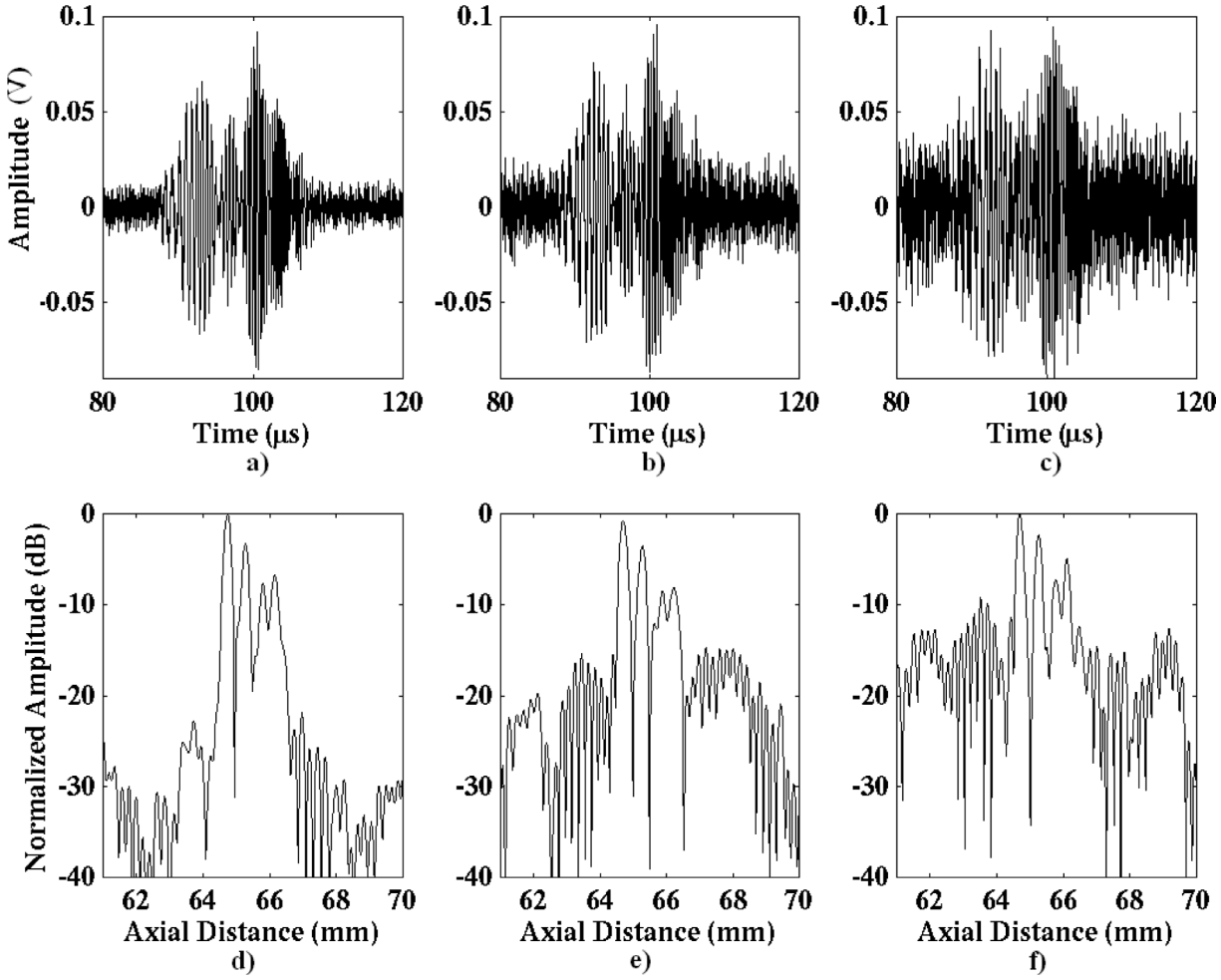

Fig. 14. (a)–(c) The waveforms backscattered from the four tungsten wires with eSNR values of 15 dB, 9 dB, and 3 dB, respectively. (d)–(f) Envelopes of the compressed waveforms of (a)–(c), respectively, using the REC technique.

V. Discussion

A pulse compression technique (REC) was used to enhance the axial resolution and bandwidth of an imaging system while also providing a significant boost in the eSNR. The goal of the study was to evaluate the REC technique for conventional ultrasonic imaging and QUS imaging through increased useable bandwidth and eSNR. The technique made use of pre-enhanced FM chirps to excite more energy in frequency bands with decreasing spectral power in the bandwidth as compared to the center frequency. Mismatched filters were used to make use of the additional energy in the frequency bands. The mismatched filters were designed based on convolution equivalence (the pre-enhanced FM chirp convolved with the source impulse response was equal to a linear FM chirp convolved with a pulse approximately twice the bandwidth of the impulse response of the source).

Simulations and experimental measurements were used to validate the REC technique in enhancing axial resolution, bandwidth, and eSNR. The simulations indicated that significant improvements in axial resolution and bandwidth could be obtained with the REC technique. Useable bandwidth, defined as +6 dB $\overline{\text{eSNR}}$, and eSNR also were increased in simulations.

Experimental measurements were conducted to verify the simulations and theory. Measurements were taken from a flat Plexiglas® reflector and from small tungsten wires. The axial resolution, −3 dB pulse/echo bandwidth, and useable bandwidth were significantly improved using the REC technique and the eSNR values of the compressed waveforms also were increased. Closely separated wires that were not resolvable with conventional pulsing techniques were resolvable with the REC technique. Long-range sidelobe levels (6 mm from the mainlobe) upon compression were more than 45 dB below the mainlobe, which is acceptable for most ultrasonic imaging purposes.

The effects of noise on the axial resolution and bandwidth enhancement also were examined. In elementary pulse compression, a trade-off between eSNR and axial resolution exists. However, the axial resolution and bandwidth enhancement was retained with lower eSNR using the REC technique. In addition, a gain in eSNR from 9.2 to 16.2 dB was achieved. The TBP product of the linear chirp used in the compression filter corresponded to a predicted gain in eSNR of 16.9 dB. The difference between

achieved gains in eSNR and predicted was attributable to the Wiener filter used in the REC technique. If a Wiener filter is used for compression, then when the eSNR is small, the Wiener filter acts like a matched filter. A matched filter would decrease the axial resolution of the system while providing the largest gain in eSNR. By increasing the bandwidth of the imaging system through the REC technique, the trade-off between gain in eSNR and axial resolution is extended over elementary pulse compression techniques. Therefore, significant gains in eSNR were achieved, although less than theoretical, with corresponding improvements in axial resolution.

The retaining of improved axial resolution over conventional pulsing with increased noise was influenced by the choice of a Wiener filter. Even with initial eSNR of 3 dB, the axial resolution was improved over conventional pulsing techniques. However, the axial resolution of the compressed waveforms with initial eSNR of 15 dB was better than the axial resolution of the compressed waveforms with initial eSNR of 3 dB; the Wiener filter behaved more like a matched filter at 3 dB eSNR and more like an inverse filter with the 15 dB eSNR waveforms. The choice of the γ parameter will play a role in the trade-off between axial resolution and eSNR. If the weighting factor were set to a larger value, the amount of gain in eSNR would increase at the cost of axial resolution and larger sidelobes. The choice of γ in the current simulations and experiments provided significant improvements in both eSNR and axial resolution. The fundamental trade-off between axial resolution and eSNR will be important depending on the application and the optimal choice of γ for specific applications has yet to be determined and will be the subject of future study. However, initial simulation and experimental results indicate that significant gains in both axial resolution and eSNR can be achieved with the REC technique.

VI. Conclusions

The preliminary study suggests that the REC technique may be a useful tool for improving QUS imaging techniques in ultrasound. Increasing the useable bandwidth of a source will improve QUS imaging techniques by reducing the variance of scatterer size estimates [14], [15]. Reduction in estimate variance due to larger useable bandwidth will extend the trade-off between QUS imaging resolution and estimate variance [22]. Furthermore, larger useable bandwidth means more information can be obtained about subresolution scatterers and multiple scales of scattering. Future studies will examine the effects of the REC technique on improving scatterer property estimates in tissue-mimicking phantoms and tissue models.

Other trade-offs may exist that were not examined in this work. To effectively implement the REC technique capabilities in QUS imaging and estimating scatterer properties, the effects of frequency-dependent attenuation also must be quantified. One effect of frequency-dependent attenuation is to reduce the TBP, thereby reducing any gain in eSNR afforded by pulse compression [23]. However, several techniques exist to mitigate some of the effects of frequency-dependent attenuation on pulse compression [24], [25].

The use of the REC technique also should be examined for additional heating of ultrasonic sources. When longer pulsing schemes are used, it is possible to heat ultrasonic sources, which could be uncomfortable or harmful to patients. When transmitting higher voltages at frequencies at which the transducer is not as efficient in converting to sound, the voltages at these frequencies are more likely to be converted to heat. However, if pulse compression techniques are being used at low enough levels to avoid nonlinear distortion, these heating effects may not be severe. Future work will examine the relationship between heating of the transducer with the REC technique and output of ultrasonic sources.

The REC technique could be useful for improving conventional ultrasonic imaging systems. To effectively implement the REC technique in conventional ultrasonic imaging, the effects on contrast resolution also should be quantified. Future work will examine the REC technique for scatterer property estimates, QUS imaging, conventional ultrasonic imaging techniques, techniques to mitigate sidelobe levels, techniques to mitigate effects of frequency-dependent attenuation, and the effects of nonlinear propagation. Trade-offs between contrast resolution and axial resolution, sidelobe level and axial resolution, and gain in eSNR and contrast resolution also will be examined.

Acknowledgments

The author would like to acknowledge the helpful discussions and technical assistance of Jie Liu, Jose Sanchez, and Michael Insana.

References

[1] F. E. Nathanson, *Radar Design Principles*. New York: McGraw-Hill, 1969.

[2] M. I. Skolnik, *Introduction to Radar Systems*. New York: McGraw-Hill, 1980.

[3] C. E. Cook and W. M. Seibert, "The early history of pulse compression radar," *IEEE Trans. Aerosp. Electron. Syst.*, vol. 24, pp. 825–833, 1988.

[4] M. O'Donnell, "Coded excitation system for improving the penetration of real-time phased-array imaging systems," *IEEE Trans. Ultrason., Ferroelect., Freq. Contr.*, vol. 39, pp. 341–351, 1992.

[5] B. Haider, P. A. Lewin, and K. E. Thomenius, "Pulse elongation and deconvolution filtering for medical ultrasonic imaging," in *Proc. IEEE Ultrason. Symp.*, 1995, pp. 1303–1308.

[6] B. Haider, P. A. Lewin, and K. E. Thomenius, "Pulse elongation and deconvolution filtering for medical ultrasonic imaging," *IEEE Trans. Ultrason., Ferroelect., Freq. Contr.*, vol. 45, pp. 98–113, 1998.

[7] J. F. Zachary, J. M. Sempsrott, L. A. Frizzell, D. G. Simpson, and W. D. O'Brien, Jr., "Superthreshold behavior and threshold estimation of ultrasound-induced lung hemorrhage in adult mice and rats," *IEEE Trans. Ultrason., Ferroelect., Freq. Contr.*, vol. 48, pp. 581–592, 2001.

[8] T. Misaridis and J. A. Jensen, "An effective coded excitation scheme based on a predistorted FM signal and an optimized digital filter," in *Proc. IEEE Ultrason. Symp.*, 1999, pp. 1589–1593.

[9] R. Y. Chiao and X. Hao, "Coded excitation for diagnostic ultrasound: A system developer's perspective," *IEEE Trans. Ultrason., Ferroelect., Freq. Contr.*, vol. 52, pp. 160–170, 2005.
[10] Y. Takeuchi, "Chirped excitation for ? 100 dB time sidelobe echo sounding," in *Proc. IEEE Ultrason. Symp.*, 1995, pp. 1309–1314.
[11] T. Misaridis and J. A. Jensen, "Use of modulated excitation signals in medical ultrasound. Part I: Basic concepts and expected benefits," *IEEE Trans. Ultrason., Ferroelect., Freq. Contr.*, vol. 52, pp. 177–191, 2005.
[12] J. Liu and M. F. Insana, "Coded pulse excitation for ultrasonic strain imaging," *IEEE Trans. Ultrason., Ferroelect., Freq. Contr.*, vol. 52, pp. 231–240, 2005.
[13] J. Liu, C. K. Abbey, and M. F. Insana, "Linear approach to axial resolution in elasticity imaging," *IEEE Trans. Ultrason., Ferroelect., Freq. Contr.*, vol. 51, pp. 716–725, 2004.
[14] P. Chaturverdi and M. F. Insana, "Error bounds on ultrasonic scatterer size estimates," *J. Acoust. Soc. Amer.*, vol. 100, pp. 392–399, 1996.
[15] M. L. Oelze, J. F. Zachary, and W. D. O'Brien, Jr., "Characterization of tissue microstructure using ultrasound backscatter: Theory and technique for optimization using a Gaussian form factor," *J. Acoust. Soc. Amer.*, vol. 112, pp. 1202–1211, 2002.
[16] R. Raman and N. Rao, "Pre-enhancement of chirp signal for inverse filtering in medical ultrasound," *Proc. 16th Annu. Conf. IEEE Eng. Med. Biol.*, pp. 676–677, 1994.
[17] S. Venkatraman and N. A. H. K. Rao, "Combining pulse compression and adaptive drive signal design to inverse filter the transducer system response and improve resolution in medical ultrasound," *Med. Biol. Eng. Comp.*, vol. 34, pp. 318–320, 1996.
[18] J. K. Tsou, J. Liu, and M. F. Insana, "Modeling and phantom studies of ultrasonic wall shear rate measurements using coded pulse excitation," *IEEE Trans. Ultrason., Ferroelect., Freq. Contr.*, vol. 53, pp. 724–734, 2006.
[19] J. Beutel, H. L. Kundel, and R. L. Van Metter, *Handbook of Medical Imaging*. Bellingham, WA: SPIE Press, 2000.
[20] M. Pollakowski, H. Ermert, L. von Bernus, and T. Schmeidl, "The optimum bandwidth of chirp signals in ultrasonic applications," *Ultrasonics*, vol. 31, pp. 417–420, 1993.
[21] T. Misaridis and J. A. Jensen, "Use of modulated excitation signals in medical ultrasound. Part II: Design and performance for medical imaging applications," *IEEE Trans. Ultrason., Ferroelect., Freq. Contr.*, vol. 52, pp. 192–207, 2005.
[22] M. L. Oelze and W. D. O'Brien, Jr., "Defining optimal axial and lateral resolution for estimating scatterer properties from volumes using ultrasound backscatter," *J. Acoust. Soc. Amer.*, vol. 115, pp. 3226–3234, 2004.
[23] N. A. H. K. Rao, "Investigation of a pulse compression technique for medical ultrasound: A simulation study," *Med. Biol. Eng. Comp.*, vol. 32, pp. 181–188, 1994.
[24] C. Passmann and H. Ermert, "A 100-MHz ultrasonic imaging system for dermatologic and ophthalmologic diagnosis," *IEEE Trans. Ultrason., Ferroelect., Freq. Contr.*, vol. 43, pp. 545–552, 1996.
[25] K. Eck, R. Schwann, A. R. Brenner, and T. G. Noll, "Depth-dependent mismatched filtering using ultrasonic attenuation as a filter design parameter," in *Proc. IEEE Ultrason. Symp.*, 1998, pp. 1639–1644.

Michael L. Oelze was born in Hamilton, New Zealand, in 1971. He earned his B.S. degree in physics and mathematics in 1994 from Harding University, Searcy, AR, his M.S. degree in physics in 1996 from the University of Louisiana at Lafayette, Lafayette, LA, and his Ph.D. degree in physics in 2000 from the University of Mississippi, Oxford, MS.

Dr. Oelze was a post-doctoral fellow at the University of Illinois at Urbana-Champaign from 2000 to 2004, conducting research in ultrasound. His research interests include the acoustic interaction with soil, ultrasound tissue characterization, quantitative ultrasound, ultrasound bioeffects, ultrasound tomography techniques, and application of coded excitation to ultrasound imaging. Currently, Dr. Oelze is an assistant professor at the University of Illinois at Urbana-Champaign.

Dr. Oelze is a member of the IEEE, the IEEE UFFC society, the American Institute for Ultrasound in Medicine, and the Acoustical Society of America.